Optimisation of a pump-as-turbine runner using a 3D inverse design methodology

Optimisation of a pump-as-turbine runner using a 3D inverse design methodology

P. Wang[1], M. Vera-Morales[1], M. Vollmer[1], M. Zangeneh[2], B. S. Zhu[3] and Z. Ma[3]

[1]Advanced Design Technology, Dilke House, 1 Malet Street, London, WC1E 7JN, United Kingdom
[2]Department of Mechanical Engineering, University College London, Torrington Place, London WC1E 7JE, United Kingdom
[3]State Key Laboratory of Hydroscience and Engineering, Department of Thermal Engineering, Tsinghua University, Beijing, 100084, China

E-mail: p.wang@adtechnology.co.uk

Abstract. In this paper the optimisation of a pump-as-turbine runner using a 3D inverse design methodology is presented. The baseline design is based on an existing runner designed with TURBOdesign1 by Zhu et al.[1, 2], that was then optimised by the genetic algorithm in Isight. In the work presented here the baseline design will be further optimised by minimizing secondary flow and profile loss factors while keeping the same meridional profile, stacking characteristics and work distribution in pump mode. The performance curves suggest that minimizing the secondary loss factor leads to an increase of the pump mode efficiency, whereas minimizing the profile loss coefficient benefits the turbine mode efficiency. These results strengthen the understanding of the trade-offs involved and provide guidelines for the design of runners for pump-as-turbine applications.

1. Introduction

The mitigation of the release of green house gas emission into the atmosphere while setting the basis for a sustainable development is one of the current society's biggest challenges. As a consequence, climate-related factors are currently driving the adaptation of the power generation and energy storage sectors. As part of the latter, pumped storage hydroelectricity is nowadays the world's largest contributor to grid energy storage, [3], and its success is based on the ability of an impeller to perform as either a pump or a turbine by reversing the direction of rotation. During the off-peak periods of electrical demand, the excess capacity generated can be used to pump water from a lower elevation reservoir into a higher elevation one. During periods of high electricity demand, the water stored at high elevation can be released through the same turbomachinery component, now working as a turbine, resulting in the production of electric power. In addition to the latter application, turbomachinery components that can be used as pumps and turbines could be used, for example, in fluid distribution units where the turbine mode can replace the pressure reducing valves, thus enabling the production of electricity.

In this paper the performance of a pump-as-turbine runner for pumped storage hydroelectricity applications is analysed with specific focus on the trade-offs between the pump and the turbine working modes. The principles of pump and turbine turbomachinery components are well known -

however, the design of components for challenging turbomachinery-based schemes like the ones explained above requires a flexible methodology that enables, for example, the exploration of trade-offs.

In this paper the optimisation of a pump-as-turbine runner using a 3D inverse design methodology is presented. The baseline design is based on an existing runner designed with TURBOdesign1 (TD1), [4], by Zhu et al. [1, 2], that was then optimised by the genetic algorithm in Isight. In the work presented here, using TURBOdesign Optima (TDOptima), [5], and keeping the same meridional profile, stacking characteristics and work distribution in pump mode, the baseline runner design will be further optimised by minimising secondary flow and profile loss factors.

2. Numerical setup

The different runner geometries were evaluated with ANSYS CFX 18.2 by solving steady-state RANS-equations with a high resolution advection scheme. The numerical set-up consists of an inlet, the runner and a vaneless section. The one-pitch hexahedral mesh used is shown in Figure 1 and contains about 500K nodes with an average y+ of 4.6. The SST model was used for the calculations and a frozen rotor interface is used between the rotating and the stationary components. For both the pump and the turbine modes the total pressure and the mass flow were applied as inlet and exit boundary conditions respectively. For the turbine mode, the flow inlet direction has been fixed to match the flow exit direction of the pump mode at design condition. As convergence criteria, the root mean square (RMS) of all solved equations should not be higher than $1x10^{-5}$. Furthermore, the variation of head and efficiency were used to judge convergence.

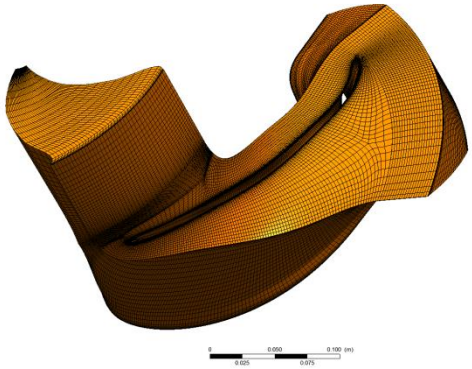

Figure 1. One-pitch hexahedral mesh.

3. Design and optimisation strategy

3.1. Baseline runner

The baseline design used in this paper is shown in Figure 2 and corresponds to Runner B from [1]. In that study, the design objectives included high efficiencies at both pump design point and turbine rated point, no cavitation at the operational range and to minimise the pressure fluctuations in the vaneless space between the runner blades and the guide vanes. The latter are identified as a likely sign of hydraulic instability. The authors analysed two optimised runners, runner A and Runner B, with significantly different lean angles, positive and negative respectively, at the high pressure side (HPS). Positive lean means the shroud leads the hub in turbine mode. These two runners have similar efficiency performance both in pump and turbine modes. However, in a subsequent paper by [2], it was concluded that the runner B, the one with negative lean, resulted in lower pressure fluctuations in the vaneless space. Their hypothesis is that this behaviour is due to the more uniform hub-to-shroud work distribution of runner B at HPS.

This paper presents the current results of an on-going study looking at the improvement of the hydraulic stability of the pump-turbine units while keeping the high values of efficiencies as well as

ensuring cavitation does not occur. The baseline runner is Runner B as described in [1] and [2], and its geometry and blade meridional profile are shown in Figure 2 (left and right respectively). While in [1] and [2] the runner is coupled with a guide vane, the results presented here focus exclusively on the runner. More details about the full stage configuration, i.e., guide vanes, stay vanes, etc., can be found in [1] and [2]. The current paper shows how the hydrodynamic performance of the runner working as both a pump and a turbine can still be improved while keeping the same meridional profile, work distribution and lean angle at HPS.

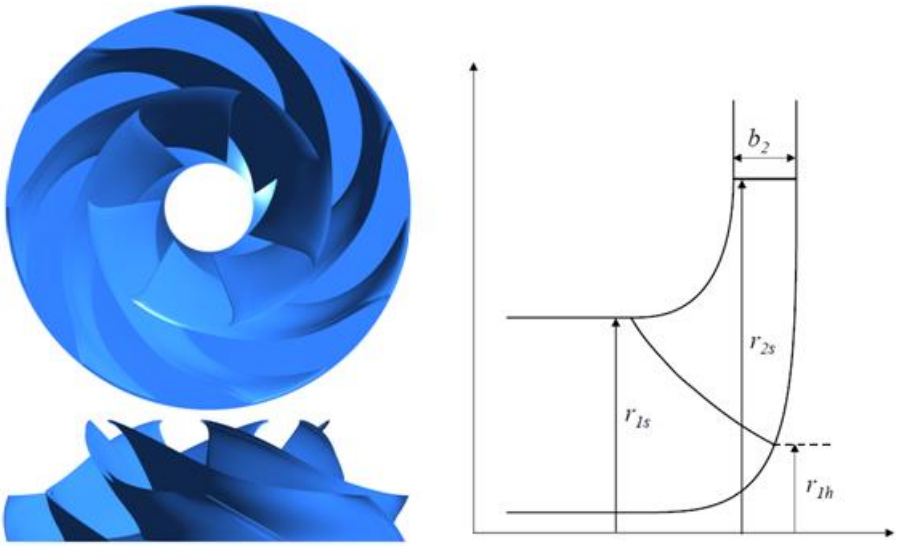

Figure 2. Runner B geometry (left) and meridional profile (right). r_{1h} = 63.5 mm, r_{1s} = 135 mm, r_2 = 224 mm, and b_2 = 51 mm.

3.2. Redesign

The blades were redesigned using TD1, a computational tool from Advanced Design Technology Ltd. (ADT), which uses a 3D inverse method to compute the blade geometry to match a specific distribution of the blade loading. TD1 generates the 3D blade shape by solving the equations for potential flow and hence the inviscid flow solution is also calculated, which can be used to assess some initial parameters. In subsection 3.2.1, two manual redesigns of the baseline will be analysed using CFX 18.2. Based on one of these two redesigns, a multi-objective optimization of the runner based on NSGA-II algorithm will be conducted using TDOptima, an ADT's in-house program that allows the user to efficiently explore a multi-factorial design space and obtain breakthrough designs, with significant performance improvements over state-of-the-art designs. As the current work focuses exclusively on the runner, the optimization will be carried out on the runner working as a pump. If the optimization had been done on the runner working as a turbine, the full stage would have had to be simulated to obtain the accurate inlet flow direction in turbine mode.

3.2.1. Manual redesign. The basic theory behind TD1 has been widely presented in literature, such as [6, 7, 8]. The runner rotational speed and volumetric flow rate used as inputs, 1000rpm and 0.281m^3/s respectively, are the same as for runner B. The input data to TD1 are the meridional geometry, the work distribution at runner exit (pump mode), the streamwise blade loading distribution, the normal blade thickness, and the specification of the blade stacking (position and angle of stacking). The streamwise blade loading distribution of the resulting redesigned runners, runner 1 (R1) and runner 2 (R2), are shown in Figure 3 as the meridional derivative of the tangential mean swirl velocity, $\partial(rV_\theta)/dm^*$, plotted versus the non-dimensional meridional distance, m^*. To validate the accuracy of

TD1 calculations, the comparison of the blade surface pressure distributions on runner R1 at the design volumetric flow rate calculated with both TD1 and CFX is shown in Figure 4. A good agreement between the two flow solvers can be seen in the figure.

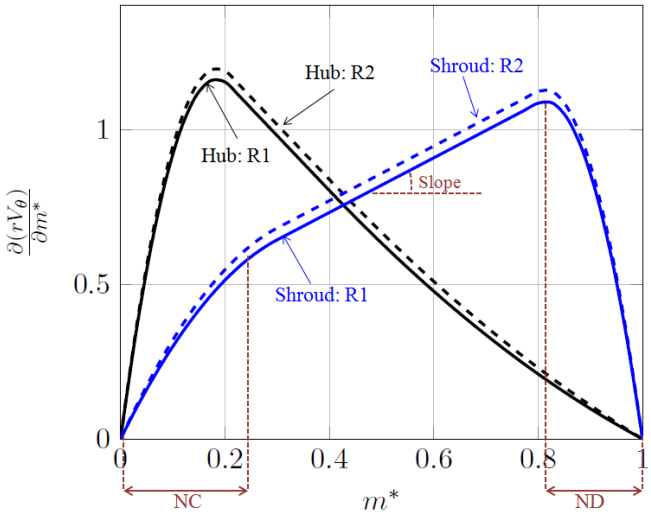

Figure 3. Streamwise blade loading distribution of manually redesigned runners.

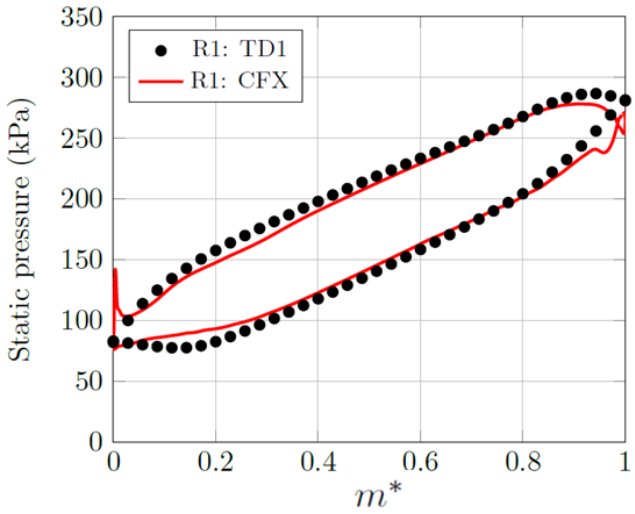

Figure 4. R1 midspan static pressure distribution calculated by TD1 and CFX.

For both R1 and R2 runners, CFD simulations were run at several volumetric flow rates. Head and efficiency comparisons between the baseline runner and the new two manually designed ones are shown in Figure 5. R1 shows a slightly lower head than the baseline design, while R2 has almost the same head performance as runner B. Additionally, R2 has a better efficiency than Runner B at high flow rates while the opposite is true at low flow rates. Due to its overall better performance, R2 was used as a starting point for the optimisation.

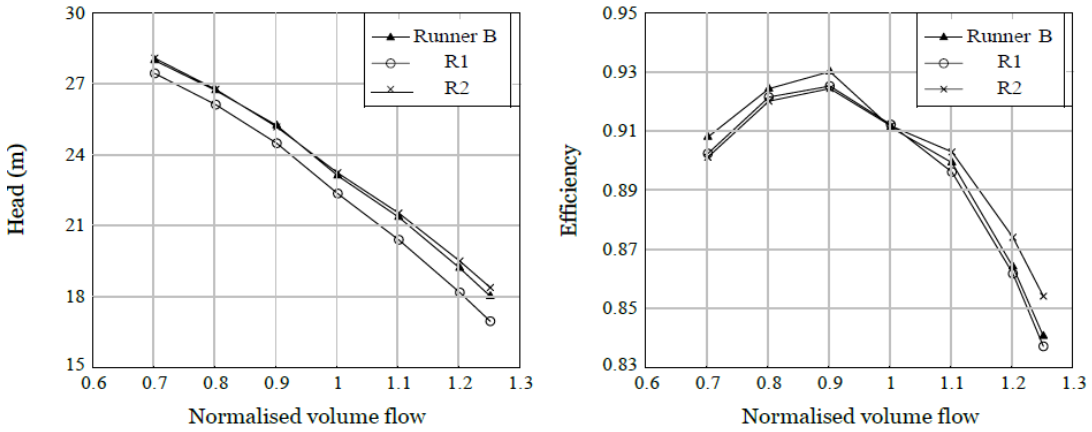

Figure 5. Comparison of baseline and manually redesigned runners performance (pump mode).

3.2.2. Optimization in TURBOdesign Optima. The fundamental methodology of optimisation in TDOptima is based on the parameterisation of the meridional housing and blade loading. In the current work the meridional geometry was not modified, and only the blade loading distributions at the hub and shroud sections were used as input (variable) parameters in TDOptima. The ranges of these input parameters are shown in Table 1.

The streamwise blade loading distribution, $\partial(rV_\theta)/dm^*$, at both hub and shroud is parameterised by means of a three-segment method, which employs a combination of two parabolic curves and an intermediate linear curve [4]. The parameters considered for this optimization are the non-dimensional streamwise location of the intersection between the first parabolic segment and the linear segment, NC, the equivalent intersection between the linear segment and the second parabolic portion, ND, and the slope of the linear segment. These parameters are indicated as an example in Figure 3.

Table 1. Input optimisation parameters for TDOptima.

	Hub		Shroud	
	min	max	min	max
NC	0.1	0.3	0.1	0.3
ND	0.4	0.85	0.4	0.85
Slope	-2.8	1	-1	1.8

In total 900 designs were generated to cover 30 generations, each of which had 30 population samples. The throat area was used as a constraint parameter to ensure the overall operating range is similar to that of the baseline. For this optimisation both the secondary flow factor (SF) and the profile loss (PL) were minimised. The definition of these parameters is given in [4]. The SF computes the driving force of meridional secondary flow on the blade suction surface, while PL is computed from the integration of cube of blade surface velocity on the true blade pressure surface. Figure 6 shows the Pareto front built from all feasible solutions of the optimization from TDOptima. The three designs chosen for further evaluation are labelled in Figure 6 as low secondary flow (R3), low profile loss (R4) and trade-off (R5) designs. The streamwise blade loading distribution at hub and shroud for each of these runners is shown in Figure 7. It is shown that the loading on the shroud section for the three new designs has been set by the optimiser to the same fore-loaded type, while the loading on the hub section is significantly different for the three designs. The runner with minimal secondary flow, R3, has a moderate aft-loaded hub loading distribution. Zangeneh et al., [9] showed that an aft-loaded hub and fore-loaded shroud can effectively reduce the secondary flow. In contrast, R4, the design with minimal profile loss, has a very strong fore-loaded streamwise loading distribution on the hub. As expected, the trade off design, R5, has a hub loading distribution somewhere in between those of R3

and R4: along the inducer hub there is a higher loading than R3 but lower than that of R4, whereas on the exducer hub the loading is less strong than R3 but stronger than that of R4.

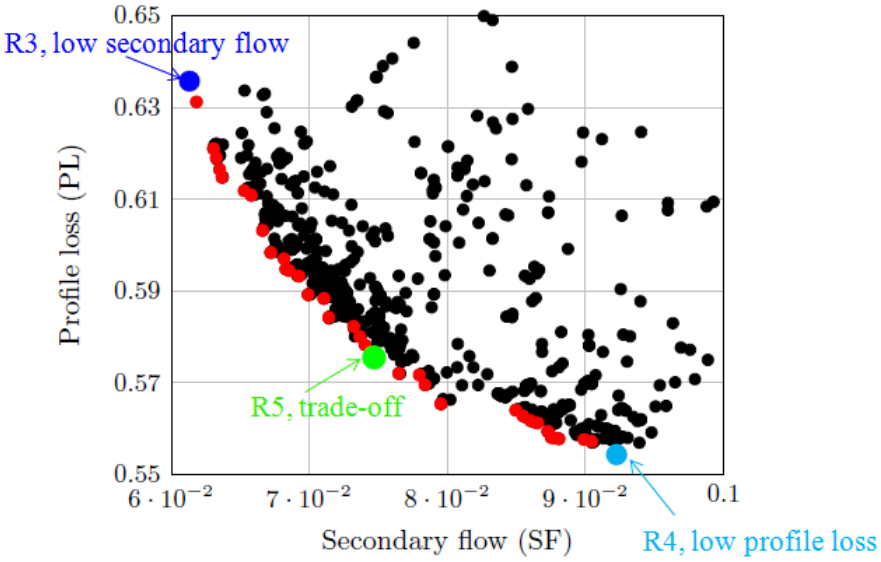

Figure 6. Pareto front on pump mode - optimisation from TDOptima.

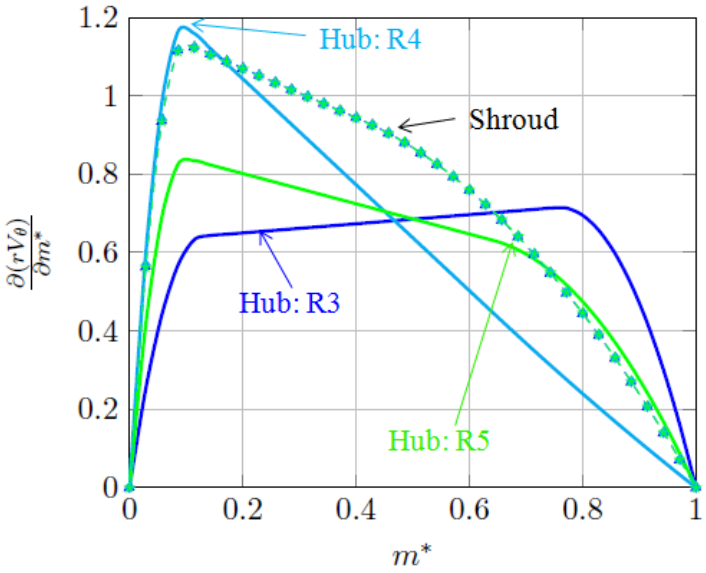

Figure 7. Blade loading distributions on pump mode.

4. CFD results

4.1. Predicted performance maps

The performance curves for the pump and turbine modes are shown in Figs. 8 and 9 respectively. When working on pump mode (Figure 8), the three designs chosen from the Pareto front achieve higher head than Runner B, with R4 obtaining the highest pump head. At higher volumetric flow rate, R3 has lower head than R4 and R5. However, R3 has higher efficiency than Runner B across the whole operating range. At design volumetric flow rate, the efficiency of R3 is about 1.6% higher than that of Runner B. It is worth noting that the design with minimal profile loss, R4, only has better efficiency than the Runner B at high volumetric flow rate. The trade off design, R5, presents a better

efficiency at high volumetric flow rate while it is worse at low volumetric flow rates. These results seem to indicate that minimising secondary flow has a benefit in the pump mode efficiency.

On turbine mode (Figure 9), R3 has a similar head performance to that of Runner B from 90% of the design flow onwards, with a lower head for lower volumetric flow rates. However, the rest of the designs have consistently lower head than Runner B. Regarding the efficiency, all three designs from TDOptima have a lower efficiency at the lowest flow rates. The design with minimal secondary flow, R3, has also less efficiency than Runner B at higher flow rates. The design with minimal profile loss, R4, has the best efficiency between 80% - 120% of the design flow. From these performance curves, it seems as if minimising profile loss has more of an effect on the turbine mode efficiency.

The comparisons above indicate that there are different dominant loss factors when the runner works as a pump or as a turbine. The trade off design may work as an overall compromising solution for the runner. In the next subsection, the detailed flow field of the different designs will be analysed.

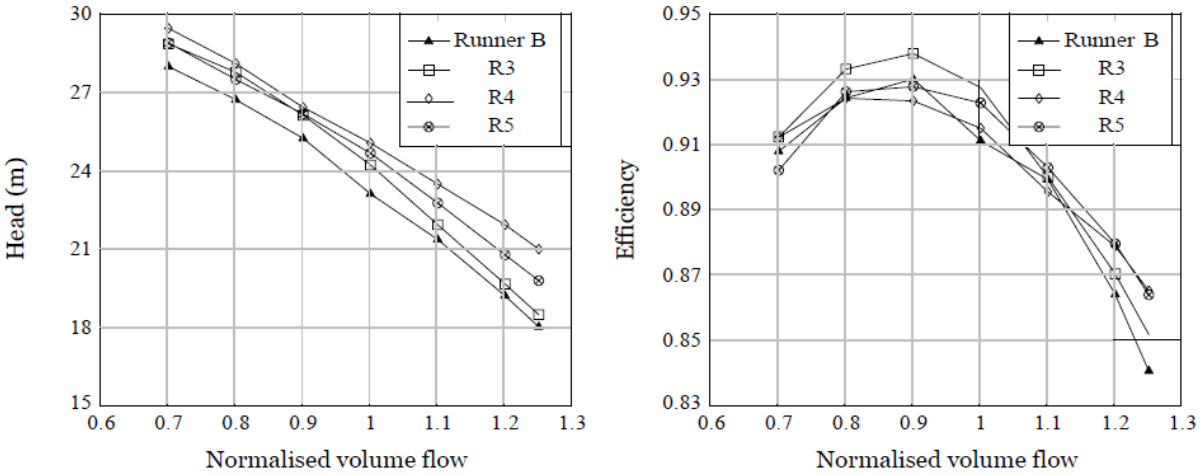

Figure 8. Head and efficiency performance of optimised runners on pump mode.

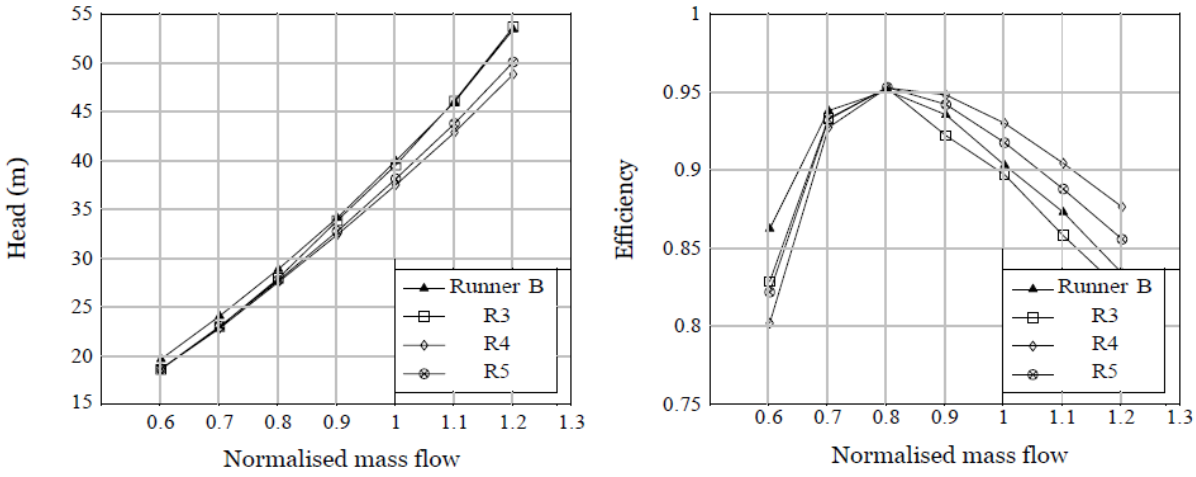

Figure 9. Head and efficiency performance of optimised runners on turbine mode.

4.2. Flow field analysis

Velocity contours at midspan and the circumferentially averaged streamwise velocity in the meridional plane for the runner working as a pump and as a turbine at design conditions are shown in Figures 10 to 13.

Figure 10 shows that towards the blades pressure side, the profile with the minimal secondary flow, R3, presents the smallest region of low momentum flow, while R4, the design with minimal profile losses, shows the largest of such regions. The trade off design, R5, features in between R3 and R4. See region labelled as A in Figure 10. This pattern correlates with the efficiency performance on pump mode at design volumetric flow rate and could imply that by minimising the secondary flow factor the area of low momentum flow towards the pressure side of the blade is reduced, contributing to a more uniform flow at the exit of the passage. This is confirmed by the circumferentially averaged streamwise velocity contours in the meridional plane, Figure 11, with R3 showing a more uniform velocity distribution than that on the other designs, especially the baseline. A small area of reverse flow is seen towards the hub inlet for all the designs, labelled as C, with that region being smaller for design R3.

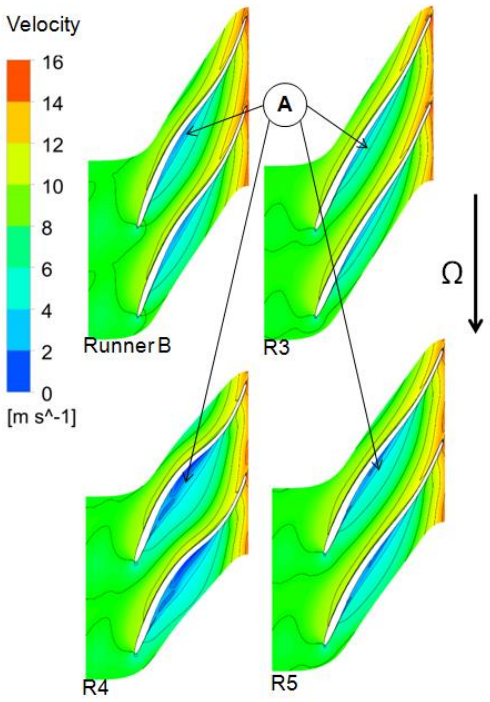

Figure 10. Velocity contours at midspan at design volumetric flow rate. Pump mode.

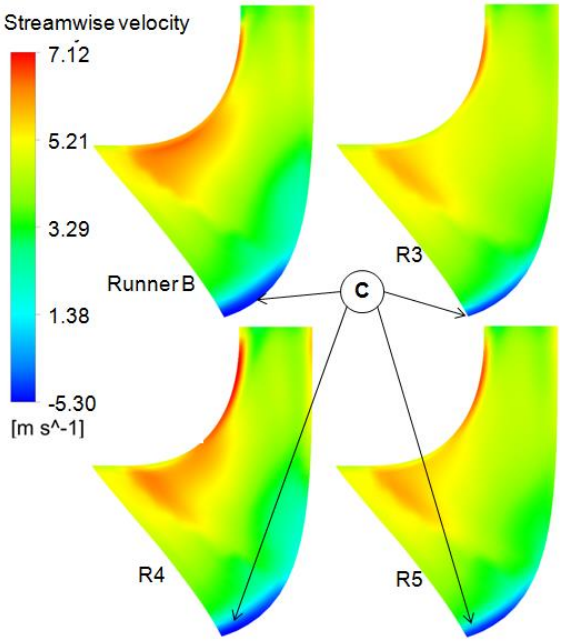

Figure 11. Circumferentially area averaged streamwise velocity in the meridional plane. Pump mode.

The corresponding figures for the runner working as a turbine are shown in Figures 12 and 13. It is worth noting that the design with minimal profile loss, R4, presents a significantly smaller flow separation on the blade suction side than the rest of the designs, see region labelled as D in Figure 12. This could affect the flow distribution along the blades and hence contribute to a lower profile loss factor. Figure 13 shows the circumferentially averaged streamwise velocity contours on the meridional plane for the turbine mode. The inlet to the turbine, or HPS, presents a change in the location of low circumferentially averaged streamwise velocity, E, between R3 and the other runners. This is due to the different streamwise loading distribution seen in Figure 7 that also affects the distribution of streamwise velocity at the exit of the turbine, i.e., the low pressure side (LPS).

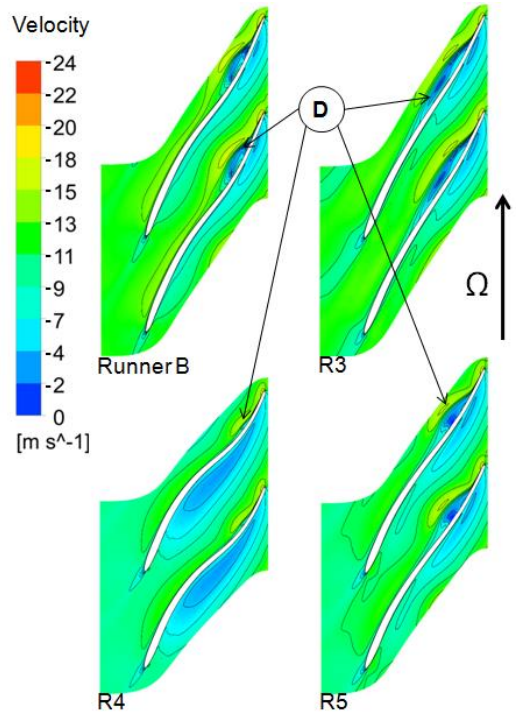

Figure 12. Velocity contours at midspan at design volumetric flow rate. Turbine mode.

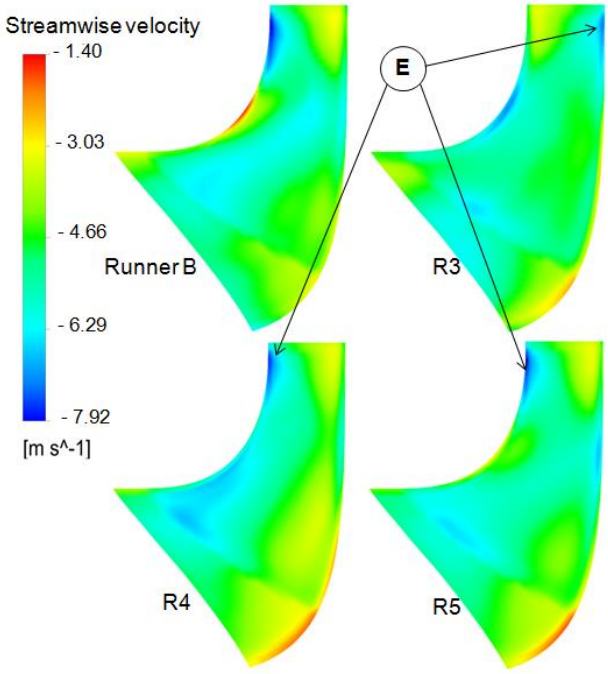

Figure 13. Circumferentially area averaged streamwise velocity in the meridional plane. Turbine mode.

5. Conclusions

In this paper we have presented a redesign and optimisation of a pump-as-turbine runner. The 3D inverse design code TD1 was first used to create a preliminary design that has a similar performance to the existing runner designed by Zhu et al. [1]. The optimisation module, TDOptima was then applied to run the multi-objective optimizations in which the targets were to minimise the TD1 secondary flow factor and the profile loss coefficient. A Pareto front was constructed and three designs were selected corresponding to minimal secondary flow, minimal profile loss and a trade-off design. These designs were analysed using CFD and the results indicate that minimising the secondary loss factor leads to an increase of the pump mode efficiency, whereas minimising the profile loss coefficient benefits the turbine mode efficiency. These results strengthen the understanding of the trade-offs involved and provided guidelines for the design of runners for pump-as-turbine applications.

Nomenclature

Acronyms	
rpm	Revolutions per minute
SST	Shear Stress Transport
Roman Symbols	
b	Impeller exit width (as pump)
m^*	Non-dimensional meridional distance
Q	Volumetric flow rate
r	Radius
V	Velocity
Greek Symbols	
Ω	Rotational speed
θ	Tangential direction component

Subscripts

h	Hub
s	Shroud
1	Inlet-Leading edge (pump mode)
2	Outlet-Trailing edge (pump mode)

References

[1] Zhu, B.S., Wang, X.H., Tan, L., Zhou, D.Y., Zhao, Y., and Cao, S.L. 2015. Optimisation Design of a Reversible Pump-turbine Runner with High E ciency and Stability. *Renewable Energy*. **Vol(81)**, pp.366-376.

[2] Zhu, B.S., Tan, L., Wang, X.H., and Ma, Z. 2018. Investigation on Flow Characteristics of Pump-Turbine Runners With Large Blade Lean. *Journal of Fluid Engineering*. **Vol(140)**, pp.031101-1-9.

[3] REN 21 Renewables Global Status Report. 2016.

[4] Advanced Design Technology Ltd.. 2018. TURBOdesign1-User Manual

[5] Advanced Design Technology Ltd.. 2018. TURBOdesign Optima-User Manual

[6] Zangeneh, M. 1991. A Compressible Three-dimensional Design Method for Radial and Mixed Flow Turbomachinery Blades. *International Journal of Numerical Methods in Fluids*. **Vol(13)**, pp.599-624.

[7] Zangeneh, M, Goto, A., and Takemura, T. 1996. Suppression of Secondary Flows in a Mixed-Flow Pump Impeller by Application of Three-Dimensional Inverse Design Method Part 1 - Design and Numerical Validation. *Journal of Turbomachinery*. **Vol(18)**, pp.536-543.

[8] Goto, A., Takemura, T, and Zangeneh, M. 1996. Suppression of Secondary Flows in a Mixed-Flow Pump Impeller by Application of Three-Dimensional Inverse Design Method Part 2 Experimental Validation. *Journal of Turbomachinery*. **Vol(18)**, pp.544-551.

[9] Zangeneh, M, Goto, A., and Harada, H. 1999. On the Role of 3D Inverse Design Methods in Turbomachinery Shape Optimization. *Proc Instn Mech Engrs.* **Vol(213)**, pp.544-551.